Natural variation of maize root hydraulic architecture underlies highly diverse water uptake capacities

Louai Rishmawi, Fabrice Bauget, Virginia Protto, Cyril Bauland, Philippe Nacry, Christophe Maurel

▶ **To cite this version:**

Louai Rishmawi, Fabrice Bauget, Virginia Protto, Cyril Bauland, Philippe Nacry, et al.. Natural variation of maize root hydraulic architecture underlies highly diverse water uptake capacities. Plant Physiology, 2023, 192 (3), pp.2404-2418. 10.1093/plphys/kiad213 . hal-04089114

HAL Id: hal-04089114
https://hal.inrae.fr/hal-04089114

Submitted on 4 May 2023

HAL is a multi-disciplinary open access archive for the deposit and dissemination of scientific research documents, whether they are published or not. The documents may come from teaching and research institutions in France or abroad, or from public or private research centers.

L'archive ouverte pluridisciplinaire **HAL**, est destinée au dépôt et à la diffusion de documents scientifiques de niveau recherche, publiés ou non, émanant des établissements d'enseignement et de recherche français ou étrangers, des laboratoires publics ou privés.

https://doi.org/10.1093/plphys/kiad213 PLANT PHYSIOLOGY 2023: 1–15

Plant Physiology®

Research Article

Natural variation of maize root hydraulic architecture underlies highly diverse water uptake capacities

Louai Rishmawi [1], Fabrice Bauget [1], Virginia Protto [1], Cyril Bauland [2], Philippe Nacry [1] and Christophe Maurel [1,*]

1 IPSiM, Univ Montpellier, CNRS, INRAE, Institut Agro, 34060 Montpellier, France
2 Université Paris-Saclay, INRAE, CNRS, AgroParisTech, GQE—Le Moulon, Gif-sur-Yvette, France

*Author for correspondence: christophe.maurel@cnrs.fr
The author responsible for distribution of materials integral to the findings presented in this article in accordance with the policy described in the Instructions for Authors (https://academic.oup.com/plphys/pages/General-Instructions) is Christophe Maurel.

Abstract

Plant water uptake is determined by the root system architecture and its hydraulic capacity, which together define the root hydraulic architecture. The current research aims at understanding the water uptake capacities of maize (*Zea mays*), a model organism and major crop. We explored the genetic variations within a collection of 224 maize inbred Dent lines and successively defined core genotype subsets to access multiple architectural, anatomical, and hydraulic parameters in the primary root (PR) and seminal roots (SR) of hydroponically grown seedlings. We found 9-, 3.5-, and 12.4-fold genotypic differences for root hydraulics (Lp_r), PR size, and lateral root size, respectively, that shaped wide and independent variations of root structure and function. Within genotypes, PR and SR showed similarities in hydraulics and, to a lesser extent, in anatomy. They had comparable aquaporin activity profiles that, however, could not be explained by aquaporin expression levels. Genotypic variations in the size and number of late meta xylem vessels were positively correlated with Lp_r. Inverse modeling further revealed dramatic genotypic differences in the xylem conductance profile. Thus, tremendous natural variation of maize root hydraulic architecture underlies a high diversity of water uptake strategies and paves the way to quantitative genetic dissection of its elementary traits.

Introduction

Water availability is one of the major limiting abiotic factors that affects photosynthesis and plant growth. Maintaining a continuous supply of water to the plant shoot is a fundamental role of roots (Maurel et al. 2010). The spatiotemporal pattern of water uptake in plants is mainly determined by the root hydraulic architecture, i.e. the spatial composition of the whole root system architecture (RSA) and of its hydraulic capacity. The different root classes that determine RSA have been proposed to play distinct roles in water uptake throughout the plant's life cycle (Doussan et al. 1998; Hochholdinger and Tuberosa 2009; Ahmed et al. 2018; Hazman and Kabil 2022). In lupine (*Lupinus* spp.) and maize (*Zea mays*) seedlings, for example, lateral roots (LR) are thought to be responsible for the majority of water uptake from the soil. In contrast, the taproot would mostly collect the water absorbed by the LR and transport it to the shoot (Zarebanadkouki et al. 2013; Ahmed et al. 2016). At later stages, when maize plants mature, the newly formed crown roots seem to have the highest water transport capacity, making them the major pathway for water uptake (Ahmed et al. 2018). Several studies have explored the intraspecific variation of RSA in maize and other species, and its response to various abiotic stresses (Dowd et al. 2020; Klein et al. 2020; Zheng et al. 2020; Zhang et al. 2021). While these variations are supposed to deeply influence root water transport, the precise links between the natural variations of RSA and the hydraulic properties of root systems are yet to be explored.

Received November 23, 2022. Accepted March 16, 2023. Advance access publication April 13, 2023
© The Author(s) 2023. Published by Oxford University Press on behalf of American Society of Plant Biologists.
This is an Open Access article distributed under the terms of the Creative Commons Attribution-NonCommercial-NoDerivs licence (https://creativecommons.org/licenses/by-nc-nd/4.0/), which permits non-commercial reproduction and distribution of the work, in any medium, provided the original work is not altered or transformed in any way, and that the work is properly cited. For commercial re-use, please contact journals.permissions@oup.com

Open Access

Downloaded from https://academic.oup.com/plphys/advance-article/doi/10.1093/plphys/kiad213/7117337 by INRA AVIGNON user on 24 April 2023

Water uptake is mediated through combined radial and axial flows. Radial water transport from the soil to the root stele depends on the anatomical and physiological properties of the concentric cell layers that shape root tissues (Steudle 2000). In particular, radial water transport is strongly controlled by aquaporins that are distributed along cellular membranes of essentially all root cells (Maurel et al. 2015; Lynch 2018). Aquaporins are membrane proteins that consist of 6 membrane-spanning α-helices and function as homo- or heterotetramers to facilitate the diffusion of water (Murata et al. 2000; Bienert et al. 2012). The activity of aquaporins is tightly controlled by their abundance and gating properties, the 2 aspects being regulated by post-translational modifications that eventually regulate the water flow (Zelazny et al. 2007; Di Pietro et al. 2013). In maize, 41 homologs define the aquaporin family and are classified into 4 subfamilies; the Plasma membrane Intrinsic Proteins (PIPs), Tonoplast Intrinsic Proteins, NOD26-like Intrinsic Proteins, and Small basic Intrinsic Proteins (Chaumont and Tyerman. 2014; Bari et al. 2018; Su et al. 2022). Besides determining cell-specific water transport properties, aquaporins play a pivotal role in the responsiveness of root hydraulics to a large variety of environmental stimuli (Alexandersson et al. 2005; Aroca et al. 2005; Hachez et al. 2006).

Several studies have shown the role of root anatomical parameters in determining water uptake capacity and profile. Besides lignification and suberization of endodermal cells, cell layer number, and organization can strongly impact root hydraulics (Enstone et al. 2003; Fan et al. 2006; Kreszies et al. 2019). Roots with more root cortical aerenchyma are associated with lower metabolic costs and thicker roots, hence greater soil exploration and eventually better yields under water deficiency (Zhu et al. 2010; Hu et al. 2014; Saengwilai et al. 2014; Klein et al. 2020). Moreover, a larger root cortical cell size or a lower number of cortical cell files can influence tissue hydraulics and are further beneficial parameters for maize drought tolerance (Chimungu et al. 2014a, 2014b). The genetic network determining the latter root feature has recently been elucidated (Ortiz-Ramirez et al. 2021).

The axial hydraulic conductivity mainly relies on the characteristics of xylem vessels and, according to Hagen–Poiseuille's law, can be locally approximated from the fourth power of vessel diameter. Yet, large conductive vessels can become more vulnerable to dysfunction due to cavitation under drought conditions (Hacke and Sperry 2001; Yang et al. 2019). Conversely, narrow vessels are less conductive but can be beneficial, as they can enhance drought tolerance by restricting water uptake and conserving soil moisture (Comas et al. 2013; Klein et al. 2020).

A number of modeling approaches have aimed at understanding the general relations between root architecture, anatomy, and hydraulics (Tron et al. 2015; Meunier et al. 2017; Couvreur et al. 2018; Boursiac et al. 2022). However, the multiple parameters that act on root hydraulic architecture have been investigated experimentally but in multiple independent species or physiological contexts. In particular, very few studies have concomitantly addressed RSA and hydraulic traits by typically comparing few genotypes exhibiting contrasting RSA (Schneider et al. 2017; Kreszies et al. 2019; Strock et al. 2021). To date, there are only rare studies that carried out an in-depth analysis on root hydraulics within a species, using a collection of 13 Arabidopsis (*Arabidopsis thaliana*) accessions or 6 rice varieties (Sutka et al. 2011; Grondin et al. 2016). Root hydraulic conductivity was tentatively associated with aquaporin expression and endodermal suberization; however, its relation to RSA and vascular anatomy and function was not investigated.

Maize is one of the most vital crops worldwide, economically and nutritionally for both humans and livestock (Revilla et al. 2022). Although maize has been recognized as a model organism since the 1900s (Hacke and Sperry 2001), the phenotypic and genetic variations in its root traits are still largely unknown (Hochholdinger et al. 2018). This study represents part of a project aimed at understanding the major parameters that regulate the hydraulic architecture of maize embryonic roots, to further explore and validate their genetic regulators. The latter will be deliberated in a separate study. The current research primarily aims at understanding the water uptake capacities and strategies present in maize roots. To this end, we explored the natural variation of root hydraulic architectures within a collection of several hundreds of genotypes. Noticeably, the distinctive embryonic maize root system, which is composed of a primary root (PR) and seminal roots (SR) that can be studied separately, provides an advantage for understanding the reciprocal relation between root architecture, anatomy, and hydraulics. Even though we investigated plants grown under standard (nonstressing) conditions, our study reveals dramatic genotypic-dependent variation in root water uptake capacity.

Results

Extensive variation of root architectural and hydraulic parameters in a maize diversity panel

We investigated the genetic variation of root hydraulic architecture in maize (*Z. mays*) using a diversity panel of 224 inbred Dent lines (Supplemental Table S1). When grown under standard hydroponic conditions, 11- to 12-d-old seedlings showed a root system composed of 2 types of axial roots, the PR and SR, each carrying their respective LR (see Supplemental Table S2 for parameter abbreviations). Since characterizing the full hydraulic architecture of hundreds of lines is technically demanding, we focused on a restricted set of parameters, including the surface area of the PR (SA_{PR}) and its LR ($SA\text{-}LR_{PR}$), the hydraulic conductivity of the PR (Lp_r) and the number of SR (SRN). The mean values of the 4 tested traits showed normal distributions (Fig. 1A to D), with marked differences between the most extreme lines, by 3.5- and 12.4-fold for SA_{PR} and $SA\text{-}LR_{PR}$, respectively (Fig. 1, A and B). A 9-fold difference in Lp_r was observed among genotypes (Fig. 1C) while SRN varied from 0 to 7 (Fig. 1D).

A principal component analysis (PCA) was performed to investigate possible correlations between the 4 variables.

Downloaded from https://academic.oup.com/plphys/advance-article/doi/10.1093/plphys/kiad213/7117337 by INRA AVIGNON user on 24 April 2023

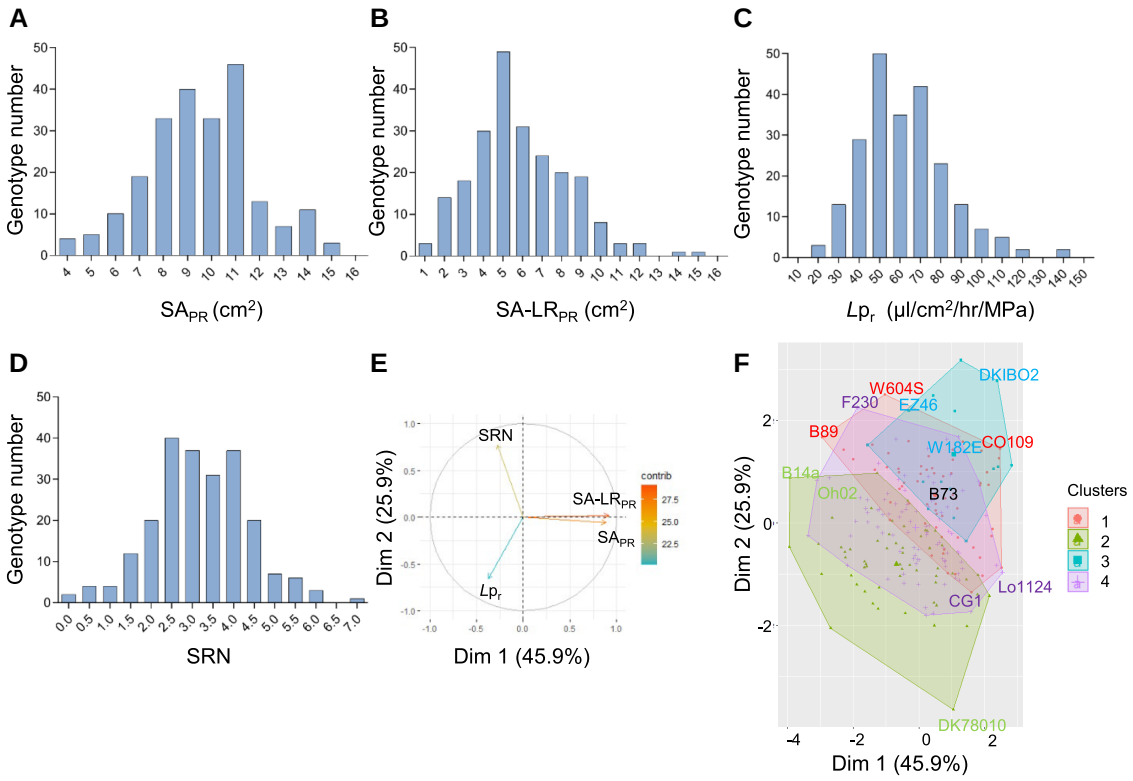

Figure 1. Frequency distribution and PCA of main RSA and hydraulic traits in a diversity panel of 224 genotypes. **A)** Frequency distribution of PR surface area (SA_{PR}). **B)** Frequency distribution of LR surface area ($SA\text{-}LR_{PR}$). **C)** Frequency distribution of PR hydraulic conductivity (Lp_r). **D)** Frequency distribution of SRN. **E)** PCA using the 4 parameters above. The figure shows the first PCA plane with position of the parameters. **F)** Cluster analysis of PCA to select contrasting genotypes. The 13 selected genotypes are highlighted on the graph, with indicated color code for the 4 clusters.

Projection along the first and second dimensions, which capture 45.9% and 25.9% of the variation, respectively, showed that PR size (SA_{PR}), PR hydraulics (Lp_r), and SR number are somewhat independent from each other (Fig. 1E; Supplemental Fig. S, 1A and B). This confirms the relevance of these few parameters to capture the genotypic diversity of root hydraulic architectures present in the panel. Yet, the surface area of the PR and its LR were highly correlated, due to synchronized growth of these 2 root types across the whole diversity panel (Fig. 1E).

To investigate in closer detail the architectural, anatomical, and molecular parameters that determine such variations in root hydraulic architecture, we decided to focus on a core subset of the aforementioned panel. An elbow method indicated that the optimal number of clusters to subclassify the population is 4 (Supplemental Fig. S2). PCA and pairwise comparisons within each cluster revealed the same correlation pattern as in the whole panel. Furthermore, we decided to select, as illustrated in Fig. 1F, 3 genotypes from each cluster (2 extremes on the cluster's edges and 1 intermediate genotype), together with the reference B73 genotype. The 13 selected lines were thereafter taken as representative of the variations present in the initial diversity panel.

Linked and independent variations of architectural and hydraulics parameters of PR and SR

An in-depth analysis of root hydraulic architecture within the core subset was performed, including a detailed characterization of the RSA and hydraulics of SR, similar to that performed for PR. Figures 2 and 3 report on the mean architectural and hydraulic parameters measured in the 13 selected lines, with variations between genotypes comparable to the maximal variations seen in the whole diversity panel. A PCA analysis using the RSA and hydraulics parameters (Lp_r) of PR and SR showed that, among the 13 genotypes, the Lp_r of PR and SR were closely linked, whereas their respective sizes (SA) were largely independent (Fig. 2C). Yet, PR size (SA_{PR}) appeared to be negatively correlated to the SRN (Fig. 2C). A linear plot of the aforementioned parameters confirmed their negative correlation (Fig. 2D). We therefore hypothesized that the emergence of SR could be controlled by an early physiological parameter, such as the amount of nutrients stored in the seed, that would be competitively used for both SR emergence and PR growth. Indeed, we observed a positive correlation between seed weight and SR number (Supplemental Fig. S3).

Detailed analysis of root hydraulic parameters indicated that genotypes that belong to the same cluster had comparable PR

Downloaded from https://academic.oup.com/plphys/advance-article/doi/10.1093/plphys/kiad213/7117337 by INRA AVIGNON user on 24 April 2023

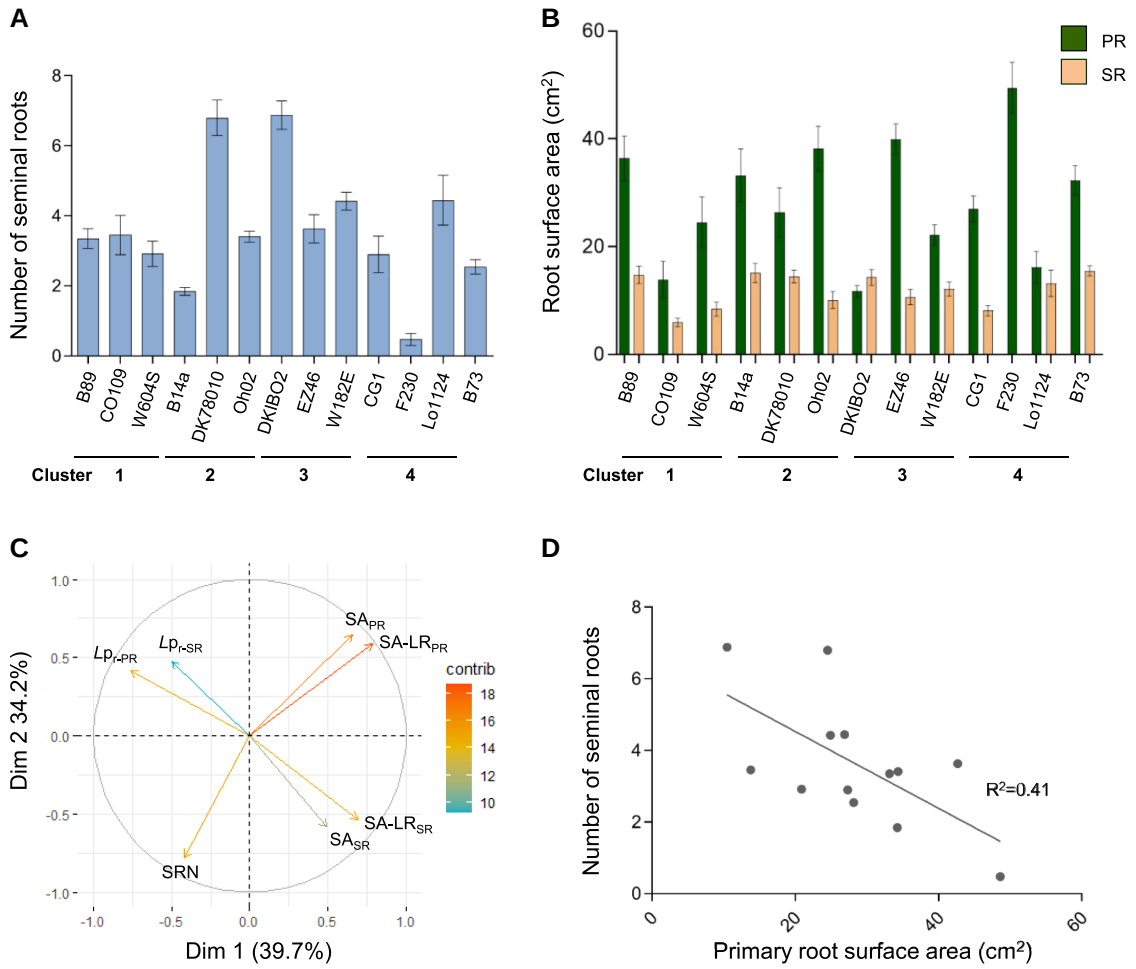

Figure 2. RSA of a core subset of 13 genotypes. **A)** SRN among the indicated genotypes and clusters. **B)** Same analysis of PR and SR surface area. **C)** PCA analysis using RSA and hydraulics parameters of PR and SR. The figure shows the first PCA plane with position of the 7 parameters analyzed. **D)** Pearson correlation study between the SA_{PR} and SRN. Each dot represents the average values of one of 13 selected genotypes. In **A** and **B)**, each of 4 clusters (see Fig. 1F) is represented by 3 adjacent genotypes, as indicated. Each bar represents the mean value (±SE) of 10 replicates.

and SR Lp_r values (Fig. 3A), a pattern that was not noticed for RSA parameters (Fig. 2, B and C). To further inspect the relation between Lp_r of PR and SR, we measured the Lp_r values of the PR and all SR in 5 selected genotypes: 1 arbitrarily chosen member from each cluster (B89, DK78010, EZ46, Lo1124) and B73 (Fig. 3B). Although the different SR of a same plant showed variation in their SA (Supplemental Fig. S4A), they had almost similar Lp_r values (Fig. 3B). Thus, each genotype exhibited a typical Lp_r that was shared between all axial roots.

The total root hydraulic conductance (L_0) represents the true water uptake capacity of a plant. It is determined by the SA and Lp_r of each axial root and its LR, and the SRN, and could be reconstructed for each of the 5 selected genotypes (Fig. 3C). The data show marked differences in L_0, up to 4-fold between EZ46 and B73 (Fig. 3C). Interestingly, DK78010 had a lower Lp_r than B73 which was compensated by a higher SRN and, therefore, a higher total root SA (Supplemental Fig. S4B). This restricted set of lines indicates that L_0 is truly diverse, due to independent genetic variations of RSA and root hydraulic parameters.

Genotypic variations of PR elementary water and solute transport parameters

To determine genuine variations of elementary water transport parameters (axial and radial conductivities) according to genotypes, we used a model-assisted workflow proposed by Boursiac et al. (2022) and recently adapted to maize (Bauget et al. 2023). In brief, we worked with PR excised from the 4 lines (Fig. 3, B and C) representing each of the 4 clusters (B89, $n = 9$; DK78010, $n = 7$; EZ46, $n = 10$; Lo1124, $n = 7$) and performed flow-to-pressure measurements in roots that were progressively cut from tip to base. Figure 4A shows how inverse modeling of such excised roots allowed to deduce the mean axial hydraulic conductance (K) profiles of each line. Although the lines exhibit differences in PR length, a dramatic increase in K was observed at ~50% of the distance from root tip to base in B89, EZ46, and Lo1124, and at ~80% in DK78010. Furthermore, EZ46 and DK78010 showed the highest and lowest K profiles, respectively, with differences by more than 1 order of magnitude. B89 and

Downloaded from https://academic.oup.com/plphys/advance-article/doi/10.1093/plphys/kiad213/7117337 by INRA AVIGNON user on 24 April 2023

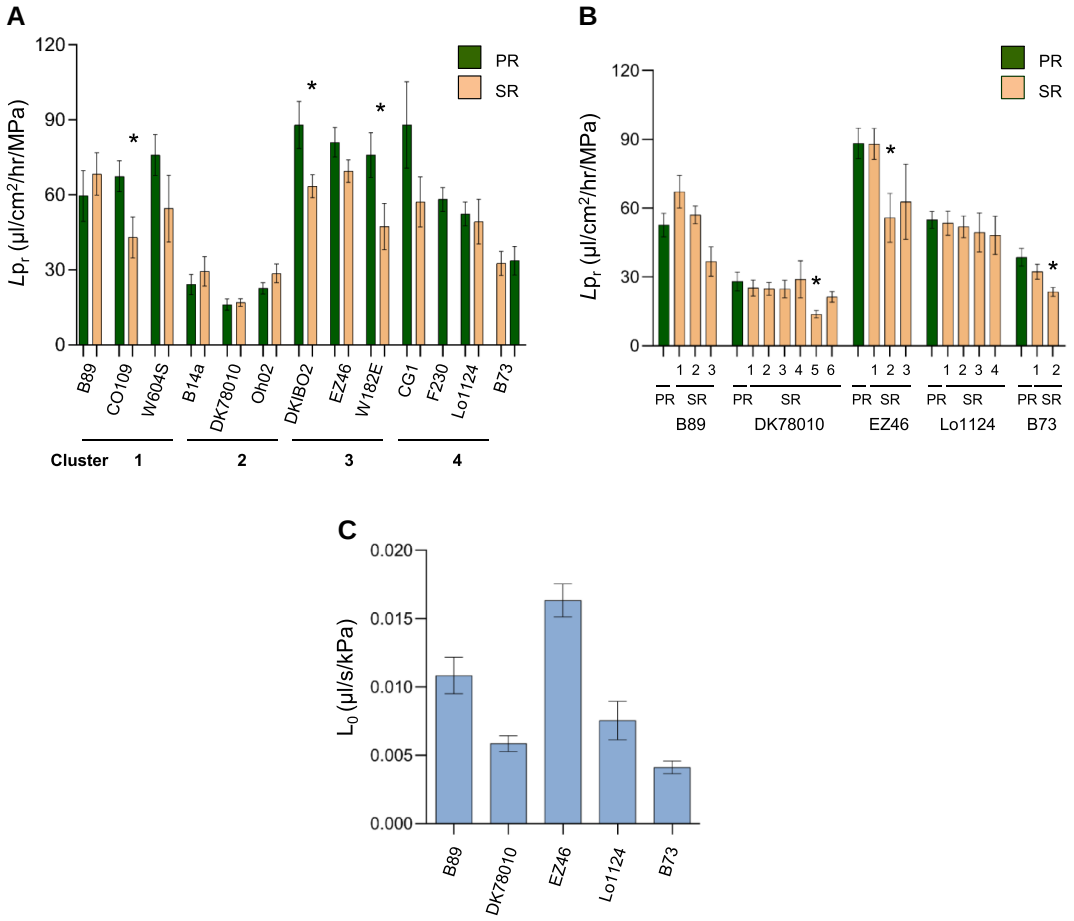

Figure 3. Characterization of hydraulics in PR and SR. **A)** Lp_r of the PR and first SR in the core subset of 13 selected genotypes. Each of 4 clusters is represented by 3 adjacent genotypes, as indicated. **B)** Detailed analysis of the Lp_r of PR and all SR of 5 further selected genotypes. Note that SR number varies between genotypes (Supplemental Fig. S4). **C)** Root hydraulic conductance (L_0) reconstructed for 5 selected genotypes. In **A)** and **B)**, asterisks (*) indicate significant differences in Lp_r between the PR and the indicated SR of the same genotype (*t*-test, *P*-value <0.05). In **A** to **C)** each bar represents the mean value (±SE) of 10 replicates, 12 replicates, and 12 replicates, for all samples except Lo1124 (8 replicates), respectively.

Lo1124 lines were intermediate but with dramatically different longitudinal profiles. However, normalizing the *x* axis (distance to tip) to take into account growth rate differences between genotypes showed that B89 and Lo1124 both exhibit an intermediate *K* over the whole distance range. These analyses provide direct evidence for genotypic differences in xylem functionality (Fig. 4A).

Solute transport parameters (Supplemental Fig. S5) and, most importantly, mean radial hydraulic conductivity (*k*) value were also determined using the same inverse modeling approach (Fig. 4B). The latter parameter showed more than 4-fold variation between lines and a similar trend as the axial conductance (*K*), with EZ46 and DK78010 having maximum and minimum *k* values, respectively, and B89 and Lo1124 intermediate values. Overall, this model-assisted determination of radial water conductivity (*k*) yields values and a genotype ranking that are somewhat consistent with those obtained in whole root Lp_r measurements (Fig. 3A). The modeling approach was also used to visualize at high resolution the hydraulic functioning of contrasting root systems. In brief, real RSAs representative of each line was digitized and the hydraulic parameters described above were used to simulate localized water inflows occurring throughout the root system. In each line, the heterogeneity of osmotic and hydrostatic driving forces throughout RSA yielded higher flows in PR vs. LR and root base vs. root tips (Fig. 4C). Although performed on only 4 lines, this comparative modeling approach provides an accurate representation and sampling of the high genetic diversity of PR hydraulic architectures present in maize (Fig. 4C).

Contribution of aquaporins to genetic variation of root hydraulics

Aquaporins play a critical role in radial water transport, thereby controlling water uptake (Maurel and Nacry 2020). In order to understand the genetic variation of PR and SR Lp_r among the 13 genotypes of the core subset, and of radial conductivity (*k*) in the PR of the 4 genotypes representing

Downloaded from https://academic.oup.com/plphys/advance-article/doi/10.1093/plphys/kiad213/7117337 by INRA AVIGNON user on 24 April 2023

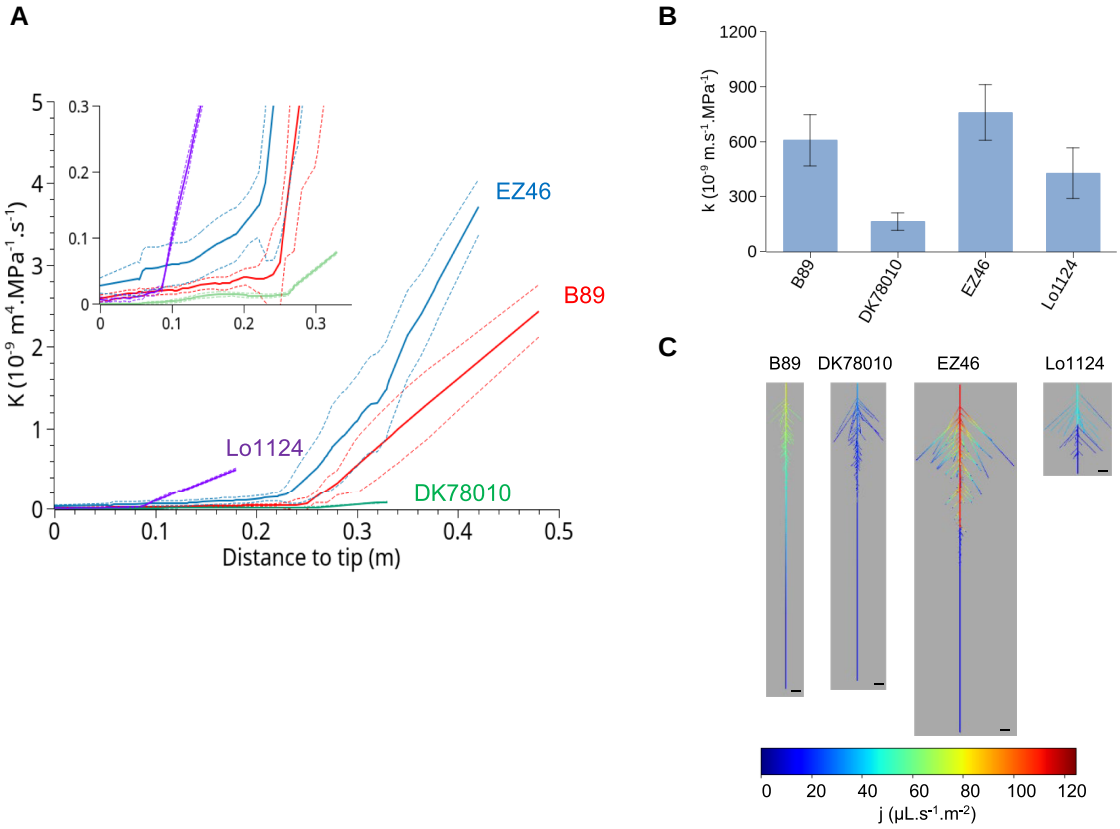

Figure 4. Inverse modeling analysis of PR hydraulics in 4 representative genotypes **A)** the figure shows variations of axial conductance (K) as a function of distance to root tip. The solid lines represent lowess fits done on K profiles of PR of B89 (red; $n = 9$), DK78010 (green; $n = 7$), EZ46 (blue; $n = 10$), and Lo1124 (purple, $n = 7$). The dashed lines delineate the corresponding 95% confidence intervals. The side panel is a detail of the main figure up to a distance to tip of 0.35 m. **B)** Averaged radial conductivity ($k \pm$ SE) of the indicated genotypes (same numbers of replicates as in **(A)**. **C)** Heat map, in representative RSAs of indicated genotypes, of local radial water flow (μL s^{-1} m^{-2}) for a pressure of 0.1 MPa. Scale bar: 10 mm.

each cluster, aquaporin activity was probed pharmacologically using the reversible blocking effects of sodium azide (NaN_3) (Sutka et al. 2011). Thirty minutes of a treatment with 1 mM NaN_3 caused a 33% to 69% reduction in the Lp_r of the PR and first SR (Fig. 5A), with rate constants in the range of 13.5 to 35.6 10^{-4} s^{-1}, meaning that Lp_r reduction was stabilized in most lines at the end of the treatment (Supplemental Fig. S6, A and B). In addition, the rate constant of Lp_r inhibition by NaN_3 was independent of the % of inhibition or the relative residual Lp_r value, suggesting that kinetic differences between lines were not linked to incomplete inhibition in some of these (Supplemental Fig. S6, C and D). With the exception of 2 genotypes (DK78010, Lo1124), the extent of Lp_r inhibition was similar in the PR and SR of each genotype but much more variable between genotypes. In particular, lines of the second cluster showed the lowest inhibition among the core subset (Fig. 5A), in accordance with their low Lp_r values (Fig. 3A) and the low k value of DK78010 (Fig. 4A). Yet, some lines with a low Lp_r, such as B73, showed a high rate of inhibition. Thus, the relative contribution of aquaporin-dependent pathways to Lp_r can show strong variations between genotypes, whereas it is pretty homogenous within the embryonic roots of each genotype.

To further dissect the contribution of aquaporins to genetic variation of Lp_r, we used qPCR and investigated the relative abundance of mRNAs of the all *ZmPIPs* in the PR and SR of the 13 genotypes. In some of these, expression of *ZmPIP2;1* and *ZmPIP2;4* mRNA could not be probed, probably due to variations in primer binding sequences. Nevertheless, all other *ZmPIPs* showed a huge genotypic variation in their relative expression levels (Fig. 5, B to D; Supplemental Fig. S7). Interestingly, expression levels of 4 of the tested *ZmPIPs* (*ZmPIP1;1*, *ZmPIP1;3*, *ZmPIP1;4*, *ZmPIP1;5*) were of comparable magnitude in PR and SR of a same genotype, in agreement with the similar Lp_r and sodium azide inhibition profiles of the 2 root types. When looking across genotypes, however, no individual *ZmPIP* showed a significant correlation between its expression and Lp_r values (Fig. 5, B to D; Supplemental Fig. S7). We conclude that, in contrast to pharmacological inhibition of aquaporins, expression levels of *ZmPIPs* at the whole root level cannot easily explain genotypic differences in Lp_r values. Yet, aquaporin expression levels may provide punctual phenotypic explanation. For instance, EZ46 exhibited the highest relative expression of most of the *ZmPIPs* in agreement with its high Lp_r value (Fig. 5, B to D; Supplemental Fig. S7).

Downloaded from https://academic.oup.com/plphys/advance-article/doi/10.1093/plphys/kiad213/7117337 by INRA AVIGNON user on 24 April 2023

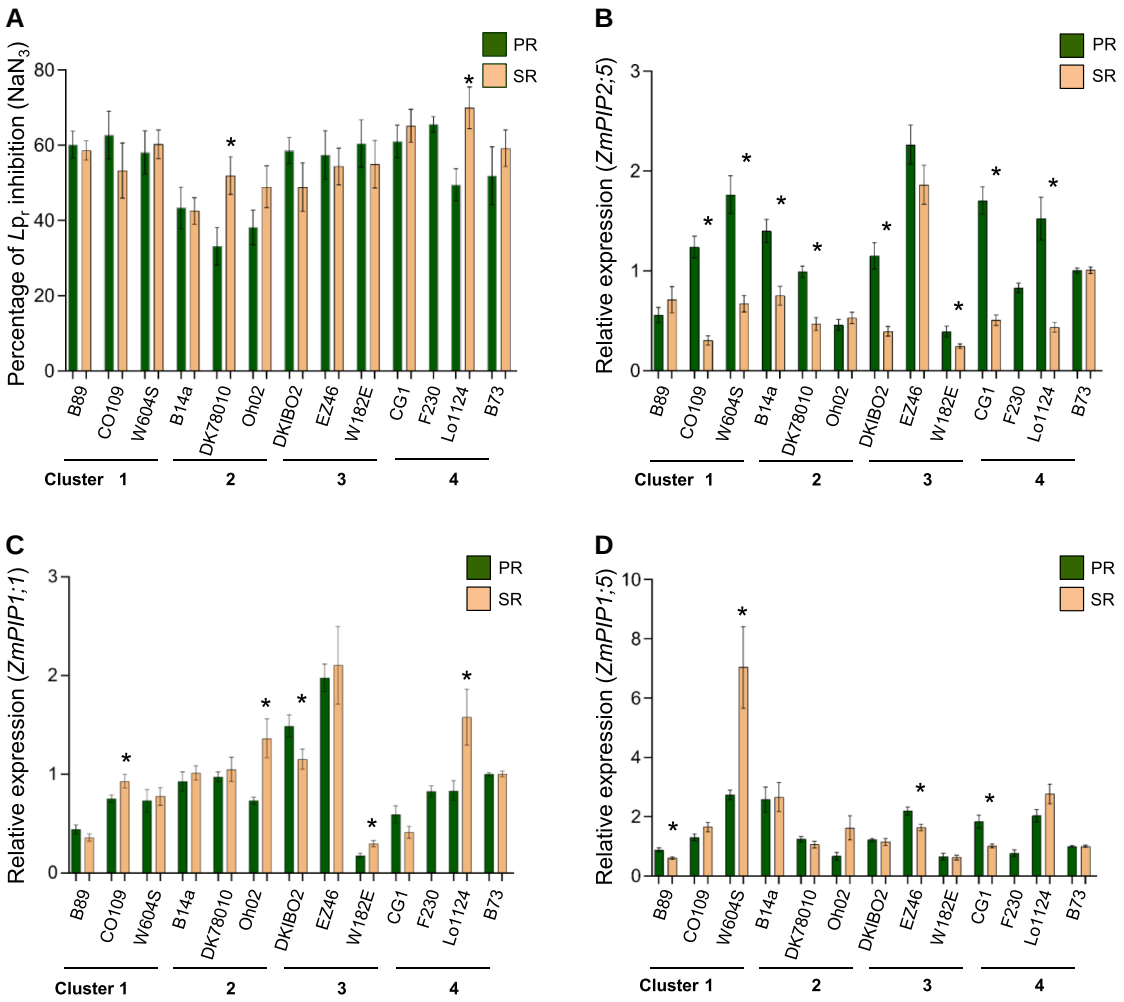

Figure 5. Contribution of aquaporins to Lp_r. **A)** Percentage (±SE) of Lp_r inhibition by NaN_3 in the PR (green) and first SR (orange) of indicated genotypes ($n = 8$ to 10). Asterisks (*) indicate significant differences in Lp_r inhibition between the PR and SR of a same genotype (*t*-test, *P*-value <0.05). **B)** Natural variation of *ZmPIP2;5* relative expression. **C)** Natural variation of *ZmPIP1;1* relative expression. **D)** Natural variation of *ZmPIP1;5* relative expression. In **B** to **D)**, the expression level of each of the *ZmPIPs* in B73 roots was set to 1 and subsequently used to calculate the relative expression level of the same gene in the 12 other genotypes. Asterisks (*) indicate a significant difference in relative expression levels between the PR (green) and SR (orange) of a same genotype (*t*-test for normally distributed data; Kolmogorov–Smirnov test for nonparametric data, *P*-value <0.05). Error bars represent SE.

Genetic variations of root anatomy and their relation to root hydraulics

Root anatomical traits (Supplemental Fig. S8) such as the thickness of the root, or of concentric tissues (stele or cortex) may influence radial water transport (k), acting on the length and tortuosity of aquaporin-dependent and -independent paths. Other traits related to vasculature anatomy (Supplemental Fig. S8) may, in contrast, determine the root axial conductance (K) profile.

Cross-sections at 7 cm from the tip of PR and SR of the 13 genotypes, that is, in the young, fully elongated part of these roots, revealed dramatic variations of all these traits (Fig. 6A). We observed, for instance, a 2.7-fold difference in the mean cross-section area between the thinnest (B14a) and thickest (Lo1124) PR (Fig. 6B). The same range of surface area difference was observed in cross-sections of the first SR (Fig. 6B). The mean number of cortical layers in PR and SR, which varied among genotypes between 6.5 (B14a) and 9.9 (F230) (Supplemental Fig. S9A) was positively correlated with the area of the PR and SR cross-sections and with LMX size (Supplemental Fig. S10, A and D), thereby explaining part of variations in root thickness.

In some genotypes (B89, CO109, W604S, DKIBO2, EZ46, CG1), the PR was thicker than the SR, whereas in all others (B14a, DK7810, Oh02, W182E, Lo1124, B73), the PR and SR had comparable thickness (Fig. 6B). In one of the latter lines (Oh02), the axial length of the PR was much higher than that of SR (Supplemental Fig. S11), indicating that, in this line, the radial growth rate of SR was somewhat higher than that of PR. Moreover, there was no correlation among the 13 genotypes between the length of PR and SR and their respective cross-section areas (Supplemental Fig.

Downloaded from https://academic.oup.com/plphys/advance-article/doi/10.1093/plphys/kiad213/7117337 by INRA AVIGNON user on 24 April 2023

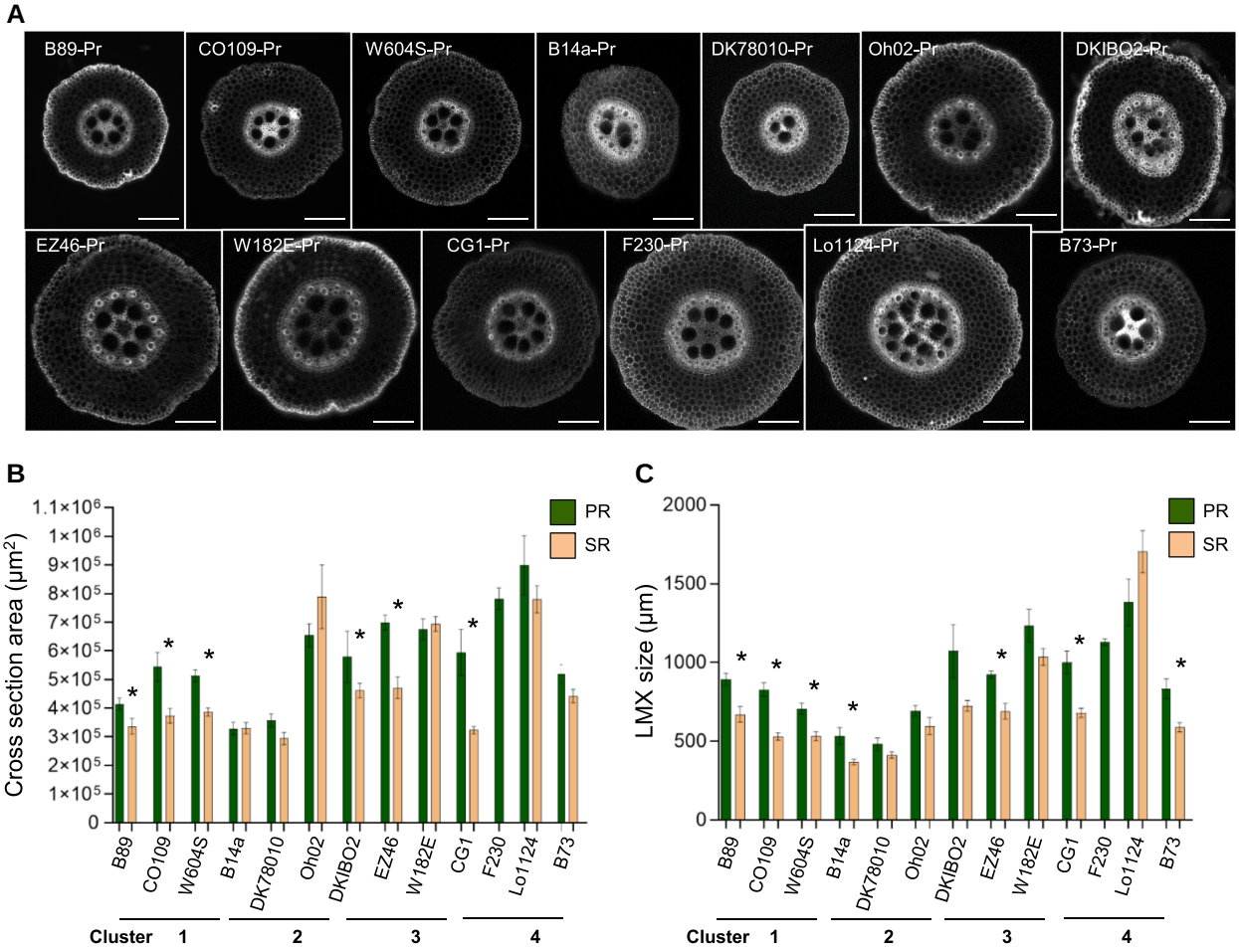

Figure 6. Natural variation of root anatomical parameters. **A)** Representative cross-sections of PR of the 13 genotypes of the core subset. Scale bars = 200 μm. **B)** Mean cross-section areas (±SE; $n = 10$ to 12) of the PR and SR of the same 13 genotypes. **C)** Mean LMZ size (±SE; $n = 10$ to 12) of the same 13 genotypes. Asterisks (*) indicate a significant difference between PR and SR of a same genotype (Kolmogorov–Smirnov test, P-value <0.05).

S10B). Thus, the thickness and length of PR and SR show largely independent genotypic variations, providing a large array of root morphological profiles (Fig. 6A). Yet, none of the traits related to root or cortex thickness was associated with Lp_r across the 13 genotypes.

We then focused on the anatomy of the stele; its area varied about 2.6-fold among the 13 genotypes (Supplemental Fig. S9B). We more specifically inspected the late meta xylem (LMX) vessels (Supplemental Fig. S8) which are potentially critical for axial water transport (Purushothaman et al. 2013; Lynch 2022). Their mean number varied in PR between 3.5 (DK78010) and 10.2 (Lo1124) and, in SR of the same lines, between 3.2 and 17.2 (Supplemental Fig. S9C). Comparable variation patterns were observed in both PR and SR for LMX vessel size (averaged radial height and width of all vessels) (Fig. 6C). When considered across genotypes, both the number and size of LMX showed a weak but statistically significant correlation with Lp_r ($R^2 = 0.36$ and $R^2 = 0.33$, respectively) (Fig. 7). This was true in particular for the extensively studied BK89, DK78010, EZ46, and Lo1124 lines (Fig. 3B). More specifically, the moderately developed vasculature observed in DK78010 (Fig. 6C; Supplemental Fig. S9, B to D) was in line with its reduced K values, as determined by inverse modeling (Fig. 4A). Yet, there was no strong link between xylem anatomical parameters at 7 cm from root tips of B89, EZ46, or Lo1124 PR and model-derived K.

In conclusion, several of root molecular and anatomical traits inspected in this study may potentially contribute to root hydraulics, thereby explaining its large genotypic diversity. In these respects, LMX anatomy appears to exert the most pronounced effects. Moreover, variations in root anatomy between the PR and SR of individual genotypes were less pronounced than variations between genotypes (Fig. 6, B to C; Supplemental Figs S9 and S12), explaining, in part, the somewhat related hydraulic properties of the 2 root types in a same genotype.

Discussion

The natural variation of maize root hydraulic architecture reveals a high plasticity of root functions

In the present work, we used the concepts of "*root hydraulic architecture*" and even "*root hydraulic anatomy*" (introduced

Downloaded from https://academic.oup.com/plphys/advance-article/doi/10.1093/plphys/kiad213/7117337 by INRA AVIGNON user on 24 April 2023

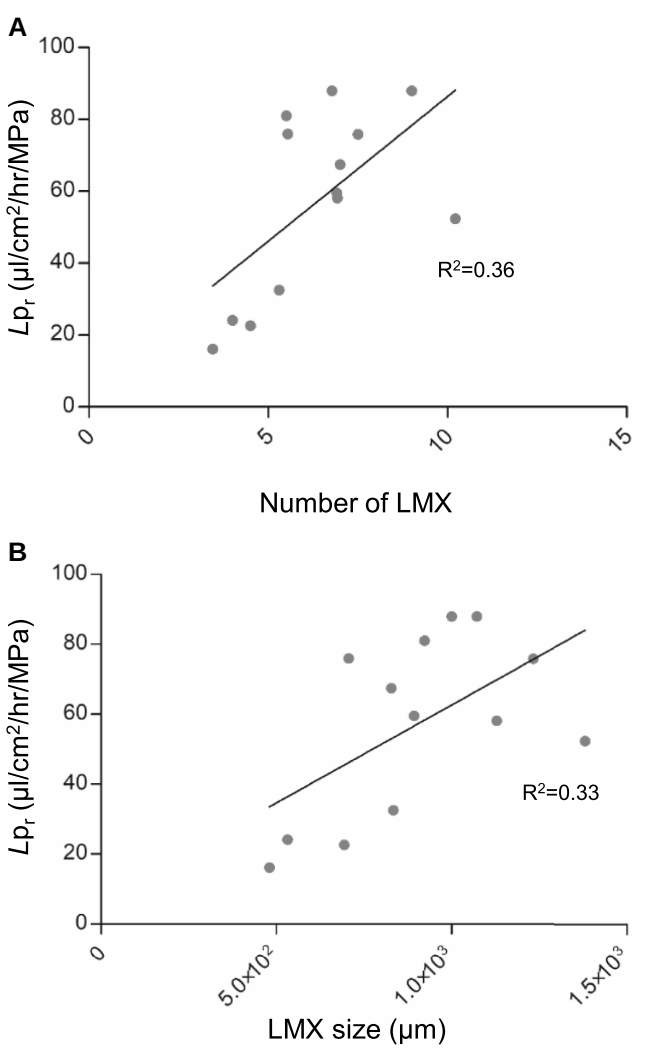

Figure 7. Relation between cross-section anatomical parameters and Lp_r. **A)** Correlation studies showing a positive correlation between Lp_r and the number of LMX. **B)** Positive correlation between LMX size and Lp_r. LMX size was calculated as the average radial height and width of individual LMX vessels. In **A)** and **B)**, each dot represents the average values of one of 13 genotypes of the core subset.

by Couvreur et al. 2018) to explore the importance of combined, intraspecific genetic variations in root architecture, anatomy, and hydraulics. With respect to previous studies made in the model dicot *A. thaliana* (Sutka et al. 2011) or rice (Grondin et al. 2016), we opted to work on maize which has a highly programmed root system development and dissected the respective roles of individual root types (e.g. PR and SR).

More specifically, we started from a whole diversity panel of 224 maize lines and delineated 4 typical clusters, each with 3 or, in some approaches, a single representative genotype. These successively defined core genotype subsets allowed a progressive refinement of our analyses and deep insights into multiple root architectural and anatomical parameters: SR number, the surface of individual PR and SR and their LR, the anatomy of their cortical and vascular tissues including size of LMX vessels were therefore considered. Concerning hydraulics, we could independently investigate the hydraulics of PR and individual SR, going down to elementary radial and axial conductances in the former root type. Aquaporin activity and expression of individual *ZmPIP* genes were determined in both PR and SR. We note that more than 2-fold variations could be observed between genotypes, for all functional, anatomic, or molecular parameters investigated.

In retrospect, the set of 4 parameters that was used to investigate the whole diversity panel, and that focused on PR RSA and hydraulics, proved to be relevant due to the correlation existing between the Lp_r of PR and SR, and to a lesser extent between PR and SR anatomy. Thus, these few parameters allowed capture of extremely broad genetic variations in root hydraulic architecture.

Our full data set more specifically revealed wide arrays of root morphologies with marked variations in both SR number and PR and SR morphology. In the latter case, we could even observe somewhat independent variations between PR and SR morphology and, within each root type, of length vs. thickness. The rationale for such huge root structure variations is not fully understood but must be linked to variations in root functions as diverse as nutrition or anchorage.

The hydraulic traits also displayed a large range of variations that were somewhat independent of RSA traits. At first sight, this might be surprising if we assume that hydraulics possibly compensates for morphological variations to achieve adequate water uptake capacities. Such a remarkable genetic diversity with regard to water uptake may have evolved to meet the constraints of extremely diverse soil and water availability conditions or water demand from the plant's aerial parts. We also conclude that the genetic regulators of root architecture and root hydraulics assort independently to permit an extensive root structure and function plasticity, yet compatible with a wide range of water uptake strategies.

Yet, we acknowledge that the comprehensive phenotyping of root hydraulic architectures that underlies this work required specific experimental conditions for plant growth and root function analyses. Firstly, plants were grown in hydroponics which we assimilate to a water-sufficient growth condition but may not accurately report on the growth pattern and function of roots in genuine soil conditions. Secondly, hydraulic phenotyping was performed on excised roots, a procedure that can lead to substantial aquaporin inhibition and Lp_r downregulation (Vandeleur et al. 2014). In this study, all lines exhibited aquaporin activities contributing to at least 35% of Lp_r (Fig. 5A) indicating that, if present, this inhibition phenomenon was partial. Yet, aquaporin activity was probed pharmacologically using a single type of sodium azide treatment. Despite these restrictions on its physiological importance, our data set provides a unique information on the dramatic natural variation of root hydraulic architecture in maize.

PR size and SRN are dependent on seed weight

Whereas RSA is undoubtedly dependent on water and nutrient availability, our study also points to a role for seed resources. Indeed, correlative analyses on a subset of

Downloaded from https://academic.oup.com/plphys/advance-article/doi/10.1093/plphys/kiad213/7117337 by INRA AVIGNON user on 24 April 2023

representative genotypes suggested that a higher seed weight would result in an increase in the SRN, in total embryonic root length (Supplemental Figs S3 and S4B) and, thereby, in root hydraulic conductance (Fig. 3C). The number and the length of SR were previously shown to be linked to nitrogen and phosphorus availability and transport (Zhu et al. 2006; Perkins and Lynch 2021). In the present work, the SRN was negatively correlated with PR size (Fig. 2D), pointing to a competition between different root types for the nutrients stored in the seed. These analyses exemplify how a critical root trait, SR number, integrates multiple internal and environmental components to shape the water and nutrient uptake capacity of the plant.

PR and SR have some similar hydraulic capacities

The PR and SR of maize are thought to play distinctive roles, due to differences in their global gene expression profiles under favorable and stress conditions (Zhang et al. 2015; Tai et al. 2016). For example, genes responsible for cell remodeling and cell wall formation and stress-related genes were more represented in PR than SR (Tai et al. 2016). Moreover, salt stress resulted in a more pronounced growth inhibition in SR than PR (Zhang et al. 2015). At variance with this idea, and even though the PR and the first SR of a same genotype exhibited distinct sizes (Supplemental Fig. S12), their hydraulic capacities were somewhat comparable (Fig. 3A). This was confirmed by detailed analysis of the whole set of SR produced in 5 selected genotypes (Fig. 3B; Supplemental Fig. S4A). Accordingly, the PR and first SR had comparable aquaporin activity profiles, as revealed using sodium azide inhibition (Tournaire-Roux et al. 2003) (Fig. 5A). In support for this, several *ZmPIPs* showed a comparable expression pattern between the 2 root types (Fig. 5, B to D; Supplemental Fig. S7). One noticeable exception was *ZmPIP2;5*, with a higher expression level in PR than SR, in 7 out of the 13 genotypes (Fig. 5B). *ZmPIP2;5* is the most highly expressed aquaporin gene in the maize root and knocking it out resulted in a marked decrease in Lp_r (Hachez et al. 2006; Ding et al. 2020). At variance with observations in Arabidopsis and rice (Sutka et al. 2011; Grondin et al. 2016), expression levels of individual *ZmPIP* genes where not indicative of whole root hydraulic properties. We realize that a more precise understanding of cell-specific expression of specific aquaporin isoforms together with understanding their post-translational regulations will be required to spatially integrate transcellular pathways throughout the maize root system. Nevertheless, our data indicate that aquaporin function is fairly well conserved within the embryonic roots of a same genotype, whereas it is highly variable between genotypes.

Root anatomy can partially account for root hydraulic properties

A precise phenotyping of root anatomy provided another dimension to address the genetic variation of radial and axial root hydraulic conductances. The most striking differences observed between genotypes were in the thickness of the root and size of the LMX, that both varied by up to 2.7-fold (Fig. 6, B and C). Root thickness, which was associated with the number of cortical layers and the stele area (Supplemental Fig. S10, A and C) did not show any clear link to Lp_r. We did not investigate root cell suberization, which can oppose radial resistance to water flow (Calvo-Polanco et al. 2021), due to the large efforts required to obtain a quantitative and thorough comparison of genotypes. Thus, our work did not allow to identify any clear anatomical component for radial conductivity, which was mostly contributed by aquaporins.

In contrast, our analyses revealed a slight positive correlation between root hydraulics and the number and size of LMX (Fig. 7). Although this correlation seems to agree with the commonly used Hagen–Poiseuille's law, several notes of caution are needed here. Firstly, LMX size was sampled at a unique distance (7 cm) from root tip whereas axial K conductance is eminently variable along root axis. Secondly, our calculation indicates that, in relation to Hagen–Poiseuille's law, S^2/n (where S is the total LMX cross-sectional area and n is the number of LMX vessels) is a more appropriate proxy for axial conductivity than vessel size. Yet, our data did not show any strong link across 13 genotypes between Lp_r and S^2/n. Thirdly, several recent studies have shown that the Hagen–Poiseuille's law does not provide an appropriate approximation of K as it neglects possible hydraulic limitations at vessel junctions or at root branching sites (Frensch and Steudle 1989; Tixier et al. 2013; Bouda et al. 2018). For these reasons, we used an inverse modeling approach to achieve a more detailed understanding of radial and axial conductances (Fig. 4). Although it had to be restricted to 4 genotypes for technical reasons, this approach pointed to a good correspondence between elementary radial conductance (k) and whole root hydraulics (Lp_r) (Figs 3 and 4). Most importantly, this approach revealed with an unprecedented resolution dramatic genotypic differences in xylem conductance profile.

Root hydraulic architecture and resistance to drought

Several of the anatomical phenotypes described in this work have been tentatively linked with drought resistance (Lynch 2018, 2022). For instance, plants with larger cortical cell size or reduced cortical cell files had a better performance under drought conditions, due to their capacity to explore the soil at reduced metabolic costs (Chimungu et al. 2014a, 2014b). In contrast, the links between xylem conductance and drought tolerance have been more disputed (reviewed by Lynch 2013). While a high xylem conductance, in root tips especially, can provide advantage for capturing residual water in drying soils (Tang et al. 2018), it can also enhance root vulnerability to cavitation or result in an early soil water exhaustion that is detrimental at terminal drought stages.

Variations in RSA have also been linked to the plant's capacity to respond to drought (Lynch 2013). For instance, maize

Downloaded from https://academic.oup.com/plphys/advance-article/doi/10.1093/plphys/kiad213/7117337 by INRA AVIGNON user on 24 April 2023

genotypes having high root system efficiency (high transpiration to root size ratio) had better yield under drought conditions (Hammer et al. 2009; van Oosterom et al. 2016). Separate experiments revealed that a reduced LR branching favors plant performance under drought (Zhan et al. 2015). Although our present study was performed with plants grown in standard hydroponic conditions, it will be instructive to further investigate the same set of 224 genotypes under water deficit conditions, to possibly identify correspondences between root water transport properties and drought tolerance (Fig. 1, A, C, and D) (Millet et al. 2016). The restricted set of lines described in this work, with highly contrasting root hydraulic architectures, provides another entry point for such studies.

Perspectives

In this study, we show that multiple root architectural, anatomical, and molecular parameters shape root hydraulic capacities and allow tremendous variations in root hydraulic architecture.

This type of study can also assist in choosing proper genotypes or ideotypes in breeding programs. As long as enhanced water uptake is needed, our work points to the possible limitation of xylem functionality and axial water transport. Yet, conducive xylem vessels may have to be coupled to high aquaporin activities, such as in EZ46, to obtain root hydraulic architectures suited to high density planting (Ren et al. 2022). In contrast, DK78010 represents, with its numerous lowly conductive SR, an interesting genotype, that may be efficient for seedling establishment and water uptake under frequent but limited rainfalls.

Characterizing the natural variation of a trait of interest can also reveal its genetic basis. Here, we chose a Dent group that was previously used for assessing the genetic variability of tolerance to various heat and drought scenarios (Millet et al. 2016). We believe that this diversity panel will be suitable for future genome wide association studies. In Arabidopsis, a 4-fold variation in Lp_r was observed among 143 accessions (Tang et al. 2018) compared to 9-fold variation in Lp_r in the current study. We are confident that future work using this population will allow the identification of genetic regulators of the root hydraulic architecture. Further comparison with genetic data obtained in the field (Millet et al. 2016) will hopefully allow to establish genetic links between root hydraulics and drought tolerance.

Materials and methods

Plant material, seed sterilization, and growth conditions

The initial phenotyping experiments relied on characterization of 6 to 8 individual plants of each of the 224 maize (*Z. mays*) inbred lines from the Amazing Dent panel (Millet et al. 2016). Subsequently, in-depth analyses were performed on the following lines: B73, DK78010, B14a, Oh02, CG1, CO109, F230, Lo1124, B89, W604S, W182E, DKIBO2, and EZ46. Unless mentioned otherwise, the different physiological, anatomical, or molecular experiments were performed with 3 technical repeats and a total of at least 10 plants per genotype. Seeds were surface sterilized with 1.5% (v/v) bleach mixed with few drops (50 to 100 μL) of Tween-20 for 5 to 8 min. The seeds were then shortly treated with 70% (v/v) of ethanol, soaked for 2 min in 35% (v/v) H_2O_2 and washed 6 times with autoclaved water. Seeds were germinated for 6 d in pots filled with wet expanded clay aggregates (Agrex 3-8, Agrex Co., Portugal). Afterwards, the germinated seedlings were transferred to a hydroponic system filled with a hydroponic solution composed of 1.25 mM KNO_3, 0.1 mM $CaCl_2$, 1.5 mM $Ca(NO_3)_2$, 0.5 mM KH_2PO_4, 0.75 mM $MgSO_4$, 0.1 mM Na_2SiO_3, 0.05 mM Fe–EDTA, 0.05 mM H_3BO_3, 0.012 mM $MnSO_4$, 0.001 mM $ZnSO_4$, 0.0007 mM $CuSO_4$, 0.00024 mM Na_2MoO_4, 0.00001 mM $CoCl_2$, and 1 mM MES. The hydroponic system was equipped with a bubbling system to ensure sufficient levels of oxygen. The seedlings were hydroponically grown for 5 to 6 d in a growth chamber at 70% relative humidity under cycles of 16 h of light (250 μmol photons m^{-2} s^{-1}) and 8 h of dark, all at 20 °C.

Root hydraulic conductance and root architecture

Root hydraulic measurements were performed essentially as described in Arabidopsis (Sutka et al. 2011). In brief, a PR or SR was excised from an individual maize plant, tightly connected to a rubber disk using a dental paste (Coltene Whaledent, France), and placed into a pressure chamber filled with hydroponic solution. The root base was then connected to a tubing device that itself is connected to high-accuracy flow meters (Bronkhorst, France). The excised root was subjected to 6 different pressures, while pressure (P)-induced sap flow (J_v) exuded from the detopped root was continuously recorded. The slope of the $J_v(P)$ curve was used to estimate the root hydraulic conductance (Boursiac et al. 2005). A WinRHIZO software (Regent Instruments Inc) was used to analyze the root architecture parameters of the scanned roots. The following parameters were considered: PR length, PR surface area, LR length, LR root surface area, and the SRN. The root hydraulic conductivity (Lp_r) was calculated by dividing the hydraulic conductance by the total surface area of the root. When indicated, excised roots were placed under constant P (0.2 MPa) in a hydroponic solution containing 1 mM NaN_3. The percentage of inhibition was calculated from the ratio of Jv at initial time and after 30 min of treatment.

Statistical analysis

All statistical analyses were conducted using GraphPad (Dotmatics, MA, USA). A Shapiro–Wilk normality test was used to test the data distribution. While a t-test was applied on normally distributed data, a Kolmogorov–Smirnov test was applied on non-normal distributed data. Linear correlation analyses (R^2) were based on genotype averages of

Downloaded from https://academic.oup.com/plphys/advance-article/doi/10.1093/plphys/kiad213/7117337 by INRA AVIGNON user on 24 April 2023

each trait. The PCA and cluster analysis were performed using the 2 R packages "FactoMineR" and "Factoextra."

RNA extraction, cDNA synthesis, and qPCR

RNA was isolated from roots of 12-d-old seedlings. TRI reagent (MRC) was added on the homogenized tissue followed by trapping and washing the RNA using a dedicated RNA extraction kit (Zymo Research) and treatment with DNASe1 (Promega). cDNA synthesis was performed using 2 μg of RNA and a GoScript reverse transcriptase (Promega). qPCR was performed as previously described (Hachez et al. 2006). Alpha-tubulin, elongation factor 1-alpha, and actin1 were used as reference genes. The expression level of each gene in B73 was used to calculate its relative expression in other genotypes. Primers used in qPCR are described in Hachez et al. (2006). Primer specificity was tested in all genotypes prior to running the qPCR. *PIP1;6* and *PIP2;6* primers did not amplify any band for CO109 and F230; *PIP1;6* primers did not amplify any band from the PR of Lo1124; *PIP2;2* primers did not work on the B89 genotype. Finally, *PIP2;1* and *PIP2;4* primers were excluded because they failed to amplify bands on most of the genotypes used in this study. The gene accession numbers of all genes used in this study and the primer sequences are indicated in Supplemental Table S3.

Root anatomy

The fixing and the clearing of PR and SR were done as previously described (Kurihara et al. 2015). Briefly, fresh roots were fixed with paraformaldehyde 4% for 1 h in a vacuum chamber, washed 2 times with phosphate-buffered saline 1%, transferred into a ClearSee solution (250 g L^{-1} urea, 100 g L^{-1} xylitol, 150 g L^{-1} sodium deoxycholate), and kept on a shaker for 5 d.

Root segments of 4 cm spanning from 5 to 9 cm from the root tip were embedded in 4% agarose placed in a special mold that was designed for preparing root cross-sections (Atkinson and Wells 2017). The middle part of the embedded root (i.e. around 7 cm from the root tip) was further used for preparing with a microtome 100 μm-thick cross-sections. Individual cross-sections were then collected with forceps, transferred to slides under a coverslip, and visualized using a axio observer (Zeiss). Phiv-Rootcell was used to estimate the cross-section parameters (number of LMX, area of LMX, LMX size, stele area, number of cortical layers), based on the autofluorescence of cell walls, as described in Lartaud et al. (2015).

Inverse modeling determination of root transport parameters

Root water and solute transport parameters were determined using the model inversion approach described by Bauget et al. (2023). The analysis was performed on the following maize inbred lines: B89, DK78010, EZ46, and Lo1124. In brief, $J_v(P)$ measurements were performed on detopped PR subjected to 11 different hydrostatic pressures in a pressure chamber. A cut-and-flow procedure was then applied, as described in details in Boursiac et al. (2022). The model used essentially corresponds to the HydroRoot functional–structural root hydraulic model (Boursiac et al. 2022) coupled with solute transport equations (Bauget et al. 2023). Water transport consists of a radial transfer, from the bathing solution to the xylem vessels, and an axial transfer along the vessels. The 2 phenomena are characterized by a radial conductivity, k (m s^{-1} MPa^{-1}), and an axial conductance, K (m^4 s^{-1} MPa^{-1}), respectively. Solute uptake consists of an active pumping, at a J_s* rate (mol s^{-1} m^{-2}), and a passive leak due to the solute concentration difference between the xylem vessels and the external medium, where P_S (m s^{-1}) is the tissue permeability. The K profile was represented as a linear piecewise function of the distance to root tip. The number of points and their abscissa correspond to the number of cuts and their distance to tip, respectively. k, J_s*, and P_s were assumed to be uniform all over the root. A reflection coefficient of 0.85 was used as in Bauget et al. (2023) where the full set of equations and all the procedures are described in details. Because they are moderately relevant for the present study and their model-assisted determination shows lower resolution (greater SE) than that of hydraulic parameters (Bauget et al. 2023), root solute transport parameters were only documented in the supplemental data.

Accession numbers

Sequence data from this article can be found in the GenBank/EMBL data libraries under accession numbers indicated in Supplemental Table S3.

Acknowledgments

We would like to thank the INRAE inbred lines gene-bank and more specifically Carine Palaffre from "CRB INRAE des lignées de maïs de Saint Martin de Hinx" for distributing the Amazing Dent panel.

Author contributions

L.R. and C.M. conceived the study. L.R. performed all of the experiments except for the modeling part. F.B. did the modeling experiment. V.P. assisted in running the experiments and in data analysis. C.B. provided the seed material. P.N. provided essential tools for running the experiments. L.R., F.B., and C.M. wrote the manuscript.

Supplemental data

The following materials are available in the online version of this article.

Supplemental Figure S1. Scree plot and variance contribution of the PCA.

Supplemental Figure S2. Elbow method to define the optimum number of clusters.

Downloaded from https://academic.oup.com/plphys/advance-article/doi/10.1093/plphys/kiad213/7117337 by INRA AVIGNON user on 24 April 2023

Supplemental Figure S3. Correlation study between seed dry weight and number of seminal roots (SRN).

Supplemental Figure S4. SA of the PR and SR of 5 selected genotypes.

Supplemental Figure S5. Averaged values of solute transport parameters as determined by inverse modeling in 4 representative genotypes.

Supplemental Figure S6. Kinetic properties of inhibition of root water transport by sodium azide.

Supplemental Figure S7. Natural variation of the relative expression of *ZmPIPs* in PR and first SR.

Supplemental Figure S8. Representative PR cross-section illustrating the measured anatomical parameters.

Supplemental Figure S9. Natural variation of anatomical parameters of PR and first SR.

Supplemental Figure S10. Correlation studies between cross-section area and other anatomical parameters.

Supplemental Figure S11. Natural variation of axial length of PR and first SR.

Supplemental Figure S12. Natural variation of total surface area of PR and first SR.

Supplemental Table S1. RSA and hydraulic phenotyping data of a diversity panel of 224 genotypes.

Supplemental Table S2. List of trait abbreviations used in this study.

Supplemental Table S3. Gene names, accession numbers and primer sequences used for gene expression studies.

Funding

This work was supported by the European Research Council (ERC) under the European Union's Horizon 2020 research and innovation programme (Grant Agreement ERC-2017-ADG-788553).

Conflict of interest statement. None declared. All authors have approved the final article.

References

Ahmed MA, Zarebanadkouki M, Kaestner A, Carminati A. Measurements of water uptake of maize roots: the key function of lateral roots. Plant Soil. 2016:**398**(1–2):59–77. https://doi.org/10.1007/s11104-015-2639-6

Ahmed MA, Zarebanadkouki M, Meunier F, Javaux M, Kaestner A, Carminati A. Root type matters: measurement of water uptake by seminal, crown, and lateral roots in maize. J Exp Bot. 2018:**69**(5):1199–1206. https://doi.org/10.1093/jxb/erx439

Alexandersson E, Fraysse L, Sjovall-Larsen S, Gustavsson S, Fellert M, Karlsson M, Johanson U, Kjellbom P. Whole gene family expression and drought stress regulation of aquaporins. Plant Mol Biol. 2005:**59**(3):469–484. https://doi.org/10.1007/s11103-005-0352-1

Aroca R, Amodeo G, Fernández-Illescas S, Herman EM, Fo C, Chrispeels MJ. The role of aquaporins and membrane damage in chilling and hydrogen peroxide induced changes in the hydraulic conductance of maize roots. Plant Physiol. 2005:**137**(1):341–353. https://doi.org/10.1104/pp.104.051045

Atkinson JA, Wells DM. An updated protocol for high throughput plant tissue sectioning. Front Plant Sci. 2017:**8** (04 October 2017):1721. https://doi.org/10.3389/fpls.2017.01721

Bari A, Farooq M, Hussain A, Tahir ul Qamar M, Abbas MW, Mustafa G, Karim A, Ahmed I, Hussain T. Genome-wide bioinformatics analysis of aquaporin gene family in maize (*Zea mays* L.). J Phylogenetics Evol Biol. 2018:**06**(2):1000197. https://doi.org/10.4172/2329-9002.1000197

Bauget F, Protto V, Pradal C, Boursiac Y, Maurel C. A root functional-structural model allows to assess effects of water deficit on water and solute transport parameters. J Exp Bot. 2023:**74**(5):1594–1608. https://doi.org/10.1093/jxb/erac471

Bienert GP, Cavez D, Besserer A, Berny MC, Gilis D, Rooman M, Chaumont F. A conserved cysteine residue is involved in disulfide bond formation between plant plasma membrane aquaporin monomers. Biochem J. 2012:**445**(1):101–111. https://doi.org/10.1042/BJ20111704

Bouda M, Brodersen C, Saiers J. Whole root system water conductance responds to both axial and radial traits and network topology over natural range of trait variation. J Theor Biol. 2018:**456** (7 November 2018):49–61. https://doi.org/10.1016/j.jtbi.2018.07.033

Boursiac Y, Chen S, Luu DT, Sorieul M, van den Dries N, Maurel C. Early effects of salinity on water transport in Arabidopsis roots. Molecular and cellular features of aquaporin expression. Plant Physiol. 2005:**139**(2):790–805. https://doi.org/10.1104/pp.105.065029

Boursiac Y, Pradal C, Bauget F, Lucas M, Delivorias S, Godin C, Maurel C. Phenotyping and modeling of root hydraulic architecture reveal critical determinants of axial water transport. Plant Physiol. 2022:**190**(2):1289–1306. https://doi.org/10.1093/plphys/kiac281

Calvo-Polanco M, Ribeyre Z, Dauzat M, Reyt G, Hidalgo-Shrestha C, Diehl P, Frenger M, Simonneau T, Muller B, Salt DE, et al. Physiological roles of Casparian strips and suberin in the transport of water and solutes. New Phytol. 2021:**232**(6):2295–2307. https://doi.org/10.1111/nph.17765

Chaumont F, Tyerman SD. Aquaporins: highly regulated channels controlling plant water relations. Plant Physiol. 2014:**164**(4):1600–1618. https://doi.org/10.1104/pp.113.233791

Chimungu JG, Brown KM, Lynch JP. Large root cortical cell size improves drought tolerance in maize. Plant Physiol. 2014a:**166**(4):2166–2178. https://doi.org/10.1104/pp.114.250449

Chimungu JG, Brown KM, Lynch JP. Reduced root cortical cell file number improves drought tolerance in maize. Plant Physiol. 2014b:**166**(4):1943–1955. https://doi.org/10.1104/pp.114.249037

Comas LH, Becker SR, Cruz VM, Byrne PF, Dierig DA. Root traits contributing to plant productivity under drought. Front Plant Sci. 2013:**4 (05 November 2013)**:442. https://doi.org/10.3389/fpls.2013.00442

Couvreur V, Faget M, Lobet G, Javaux M, Chaumont F, Draye X. Going with the flow: multiscale insights into the composite nature of water transport in roots. Plant Physiol. 2018:**178**(4):1689–1703. https://doi.org/10.1104/pp.18.01006

Ding L, Milhiet T, Couvreur V, Nelissen H, Meziane A, Parent B, Aesaert S, Van Lijsebettens M, Inze D, Tardieu F, et al. Modification of the expression of the aquaporin ZmPIP2;5 affects water relations and plant growth. Plant Physiol. 2020:**182**(4):2154–2165. https://doi.org/10.1104/pp.19.01183

Di Pietro M, Vialaret J, Li GW, Hem S, Prado K, Rossignol M, Maurel C, Santoni V. Coordinated post-translational responses of aquaporins to abiotic and nutritional stimuli in Arabidopsis roots. Mol Cell Proteomics. 2013:**12**(12):3886–3897. https://doi.org/10.1074/mcp.M113.028241

Doussan C, Page C, Vercambre G. Modelling of the hydraulic architecture of root systems: an integrated approach to water absorption-model description. Ann Bot. 1998:**81**(2):213–223. https://doi.org/10.1006/anbo.1997.0540

Dowd TG, Braun DM, Sharp RE. Maize lateral root developmental plasticity induced by mild water stress. II: Genotype-specific spatiotemporal effects on determinate development. Plant Cell Environ. 2020:**43**(10):2409–2427. https://doi.org/10.1111/pce.13840

Enstone DE, Peterson CA, Ma F. Root endodermis and exodermis: structure, function, and responses to the environment. J Plant

Downloaded from https://academic.oup.com/plphys/advance-article/doi/10.1093/plphys/kiad213/7117337 by INRA AVIGNON user on 24 April 2023

Growth Regul. 2003:**21**(4):335–351. https://doi.org/10.1007/s00344-003-0002-2

Fan L, Linker R, Gepstein S, Tanimoto E, Yamamoto R, Neumann PM. Progressive inhibition by water deficit of cell wall extensibility and growth along the elongation zone of maize roots is related to increased lignin metabolism and progressive stelar accumulation of wall phenolics. Plant Physiol. 2006:**140**(2):603–612. https://doi.org/10.1104/pp.105.073130

Frensch J, Steudle E. Axial and radial hydraulic resistance to roots of maize (*Zea mays* L.). Plant Physiol. 1989:**91**(2):719–726. https://doi.org/10.1104/pp.91.2.719

Grondin A, Mauleon R, Vadez V, Henry A. Root aquaporins contribute to whole plant water fluxes under drought stress in rice (*Oryza sativa* L.). Plant Cell Environ. 2016:**39**(2):347–365. https://doi.org/10.1111/pce.12616

Hachez C, Moshelion M, Zelazny E, Cavez D, Chaumont F. Localization and quantification of plasma membrane aquaporin expression in maize primary root: a clue to understanding their role as cellular plumbers. Plant Mol Biol. 2006:**62**(1–2):305–323. https://doi.org/10.1007/s11103-006-9022-1

Hacke UG, Sperry JS. Functional and ecological xylem anatomy. Perspect Plant Ecol Evol Syst. 2001:**4**(2):97–115. https://doi.org/10.1078/1433-8319-00017

Hammer GL, Dong ZS, McLean G, Doherty A, Messina C, Schussler J, Zinselmeier C, Paszkiewicz S, Cooper M. Can changes in canopy and/or root system architecture explain historical maize yield trends in the US corn belt? Crop Sci. 2009:**49**(1):299–312. https://doi.org/10.2135/cropsci2008.03.0152

Hazman MY, Kabil FF. Maize root responses to drought stress depend on root class and axial position. J Plant Res. 2022:**135**(1):105–120. https://doi.org/10.1007/s10265-021-01348-7

Hochholdinger F, Tuberosa R. Genetic and genomic dissection of maize root development and architecture. Curr Opin Plant Biol. 2009:**12**(2):172–177. https://doi.org/10.1016/j.pbi.2008.12.002

Hochholdinger F, Yu P, Marcon C. Genetic control of root system development in maize. Trends Plant Sci. 2018:**23**(1):79–88. https://doi.org/10.1016/j.tplants.2017.10.004

Hu B, Henry A, Brown KM, Lynch JP. Root cortical aerenchyma inhibits radial nutrient transport in maize (*Zea mays*). Ann Bot. 2014:**113**(1):181–189. https://doi.org/10.1093/aob/mct259

Klein SP, Schneider HM, Perkins AC, Brown KM, Lynch JP. Multiple integrated root phenotypes are associated with improved drought tolerance. Plant Physiol. 2020:**183**(3):1011–1025. https://doi.org/10.1104/pp.20.00211

Kreszies T, Eggels S, Kreszies V, Osthoff A, Shellakkutti N, Baldauf JA, Zeisler-Diehl VV, Hochholdinger F, Ranathunge K, Schreiber L. Seminal roots of wild and cultivated barley differentially respond to osmotic stress in gene expression, suberization, and hydraulic conductivity. Plant Cell Environ. 2019:**43**(2):344–357. https://doi.org/10.1111/pce.13675

Kurihara D, Mizuta Y, Sato Y, Higashiyama T. ClearSee: a rapid optical clearing reagent for whole-plant fluorescence imaging. Development. 2015:**142**(23):4168–4179. https://doi.org/10.1242/dev.127613

Lartaud M, Perin C, Courtois B, Thomas E, Henry S, Bettembourg M, Divol F, Lanau N, Artus F, Bureau C, et al. PHIV-RootCell: a supervised image analysis tool for rice root anatomical parameter quantification. Front Plant Sci. 2015:**5 (19 January 2015)**:790. https://doi.org/10.3389/fpls.2014.00790

Lynch JP. Steep, cheap and deep: an ideotype to optimize water and N acquisition by maize root systems. Ann Bot. 2013:**112**(2):347–357. https://doi.org/10.1093/aob/mcs293

Lynch JP. Rightsizing root phenotypes for drought resistance. J Exp Bot. 2018:**69**(13):3279–3292. https://doi.org/10.1093/jxb/ery048

Lynch JP. Harnessing root architecture to address global challenges. Plant J. 2022:**109**(2):415–431. https://doi.org/10.1111/tpj.15560

Maurel C, Boursiac Y, Luu DT, Santoni V, Shahzad Z, Verdoucq L. Aquaporins in plants. Physiol Rev. 2015:**95**(4):1321–1358. https://doi.org/10.1152/physrev.00008.2015

Maurel C, Nacry P. Root architecture and hydraulics converge for acclimation to changing water availability. Nat Plants. 2020:**6**(7):744–749. https://doi.org/10.1038/s41477-020-0684-5

Maurel C, Simonneau T, Sutka M. The significance of roots as hydraulic rheostats. J Exp Bot. 2010:**61**(12):3191–3198. https://doi.org/10.1093/jxb/erq150

Meunier F, Couvreur V, Draye X, Vanderborght J, Javaux M. Towards quantitative root hydraulic phenotyping: novel mathematical functions to calculate plant-scale hydraulic parameters from root system functional and structural traits. J Math Biol. 2017:**75**(5):1133–1170. https://doi.org/10.1007/s00285-017-1111-z

Millet EJ, Welcker C, Kruijer W, Negro S, Coupel-Ledru A, Nicolas SD, Laborde J, Bauland C, Praud S, Ranc N, et al. Genome-wide analysis of yield in Europe: allelic effects vary with drought and heat scenarios. Plant Physiol. 2016:**172**(2):749–764. https://doi.org/10.1104/pp.16.00621

Murata K, Mitsuoka K, Hirai T, Walz T, Agre P, Heymann JB, Engel A, Fujiyoshi Y. Structural determinants of water permeation through aquaporin-1. Nature. 2000:**407**(6804):599–605. https://doi.org/10.1038/35036519

Ortiz-Ramírez C, Guillotin B, Xu X, Rahni R, Zhang S, Yan Z, Coqueiro Dias Araujo P, Demesa-Arevalo E, Lee L, Van Eck J, et al. Ground tissue circuitry regulates organ complexity in maize and *Setaria*. Science. 2021:**374**(6572):1247–1252. https://doi.org/10.1126/science.abj2327

Perkins AC, Lynch JP. Increased seminal root number associated with domestication improves nitrogen and phosphorus acquisition in maize seedlings. Ann Bot. 2021:**128**(4):453–468. https://doi.org/10.1093/aob/mcab074

Purushothaman R, Zaman-Allah M, Mallikarjuna N, Pannirselvam R, Krishnamurthy L, Gowda CLL. Root anatomical traits and their possible contribution to drought tolerance in grain legumes. Plant Prod Sci. 2013:**16**(1):1–8. https://doi.org/10.1626/pps.16.1

Ren W, Zhao L, Liang J, Wang L, Chen L, Li P, Liu Z, Li X, Zhang Z, Li J, et al. Genome-wide dissection of changes in maize root system architecture during modern breeding. Nat Plants. 2022:**8**(12):1408–1422. https://doi.org/10.1038/s41477-022-01274-z

Revilla P, Alves ML, Andelkovic V, Balconi C, Dinis I, Mendes-Moreira P, Redaelli R, Ruiz de Galarreta JI, vaz Patto MC, Zilic S, et al. Traditional foods from maize (*Zea mays* L.) in Europe. Front Nutr. 2022:**8 (07 January 2022)**:683399. https://doi.org/10.3389/fnut.2021.683399

Saengwilai P, Nord EA, Chimungu JG, Brown KM, Lynch JP. Root cortical aerenchyma enhances nitrogen acquisition from low-nitrogen soils in maize. Plant Physiol. 2014:**166**(2):726–735. https://doi.org/10.1104/pp.114.241711

Schneider HM, Wojciechowski T, Postma JA, Brown KM, Lücke A, Zeisler V, Schreiber L, Lynch JP. Root cortical senescence decreases root respiration, nutrient content and radial water and nutrient transport in barley. Plant Cell Environ. 2017:**40**(8):1392–1408. https://doi.org/10.1111/pce.12933

Steudle E. Water uptake by roots: effects of water deficit. J Exp Bot. 2000:**51**(350):1531–1542. https://doi.org/10.1093/jexbot/51.350.1531

Strock CF, Burridge JD, Niemiec MD, Brown KM, Lynch JP. Root metaxylem and architecture phenotypes integrate to regulate water use under drought stress. Plant Cell Environ. 2021:**44**(1):49–67. https://doi.org/10.1111/pce.13875

Su Y, Liu Z, Sun J, Wu C, Li Y, Zhang C, Zhao L. Genome-wide identification of maize aquaporin and functional analysis during seed germination and seedling establishment. Front Plant Sci. 2022:**13 (27 January 2022)**:831916. https://doi.org/10.3389/fpls.2022.831916

Sutka M, Li G, Boudet J, Boursiac Y, Doumas P, Maurel C. Natural variation of root hydraulics in Arabidopsis grown in normal and salt-stressed conditions. Plant Physiol. 2011:**155**(3):1264–1276. https://doi.org/10.1104/pp.110.163113

Tai H, Lu X, Opitz N, Marcon C, Paschold A, Lithio A, Nettleton D, Hochholdinger F. Transcriptomic and anatomical complexity of

Downloaded from https://academic.oup.com/plphys/advance-article/doi/10.1093/plphys/kiad213/7117337 by INRA AVIGNON user on 24 April 2023

primary, seminal, and crown roots highlight root type-specific functional diversity in maize (*Zea mays* L.). J Exp Bot. 2016:**67**(4): 1123–1135. https://doi.org/10.1093/jxb/erv513

Tang N, Shahzad Z, Lonjon F, Loudet O, Vailleau F, Maurel C. Natural variation at XND1 impacts root hydraulics and trade-off for stress responses in Arabidopsis. Nat Commun. 2018:**9**(1):3884. https://doi.org/10.1038/s41467-018-06430-8

Tixier A, Cochard H, Badel E, Dusotoit-Coucaud A, Jansen S, Herbette S. *Arabidopsis thaliana* as a model species for xylem hydraulics: does size matter? J Exp Bot. 2013:**64**(8):2295–2305. https://doi.org/10.1093/jxb/ert087

Tournaire-Roux C, Sutka M, Javot H, Gout E, Gerbeau P, Luu D T, Bligny R, Maurel C. Cytosolic pH regulates root water transport during anoxic stress through gating of aquaporins. Nature. 2003:**425-**(6956):393–397. https://doi.org/10.1038/nature01853

Tron S, Perona P, Gorla L, Schwarz M, Laio F, Ridolfi L. The signature of randomness in riparian plant root distributions. Geophys Res Lett. 2015:**42**(17):7098–7106. https://doi.org/10.1002/2015GL064857

Vandeleur RK, Sullivan W, Athman A, Jordans C, Gilliham M, Kaiser BN, Tyerman SD. Rapid shoot-to-root signalling regulates root hydraulic conductance via aquaporins. Plant Cell Environ. 2014:**37**(2): 520–538. https://doi.org/10.1111/pce.12175

van Oosterom EJ, Yang Z, Zhang F, Deifel KS, Cooper M, Messina CD, Hammer GL. Hybrid variation for root system efficiency in maize: potential links to drought adaptation. Funct Plant Biol. 2016:**43**(6):502–511. https://doi.org/10.1071/FP15308

Yang JT, Schneider HM, Brown KM, Lynch JP. Genotypic variation and nitrogen stress effects on root anatomy in maize are node specific. J Exp Bot. 2019:**70**(19):5311–5325. https://doi.org/10.1093/jxb/erz293

Zarebanadkouki M, Kim YX, Carminati A. Where do roots take up water? Neutron radiography of water flow into the roots of transpiring plants growing in soil. New Phytol. 2013:**199**(4): 1034–1044. https://doi.org/10.1111/nph.12330

Zelazny E, Borst J W, Lanie Muylaert M, Batoko H, Hemminga MA, Chaumont F. FRET Imaging in living maize cells reveals that plasma membrane aquaporins interact to regulate their subcellular localization. Proc Natl Acad Sci U S A. 2007:**104**(30):12359–12364. https://doi.org/10.1073/pnas.0701180104

Zhan A, Schneider H, Lynch JP. Reduced lateral root branching density improves drought tolerance in maize. Plant Physiol. 2015:**168**(4): 1603–1615. https://doi.org/10.1104/pp.15.00187

Zhang M, Kong X, Xu X, Li C, Tian H, Ding Z. Comparative transcriptome profiling of the maize primary, crown and seminal root in response to salinity stress. PLoS One. 2015:**10**(3):e0121222. https://doi.org/10.1371/journal.pone.0121222

Zhang L, Yan M, Ren Y, Chen Y, Zhang S. Zinc regulates the hydraulic response of maize root under water stress conditions. Plant Physiol Biochem. 2021:**159(February 2021)**:123–134. https://doi.org/10.1016/j.plaphy.2020.12.014

Zheng Z, Hey S, Jubery T, Liu H, Yang Y, Coffey L, Miao C, Sigmon B, Schnable JC, Hochholdinger F, et al. Shared genetic control of root system architecture between *Zea mays* and *Sorghum bicolor*. Plant Physiol. 2020:**182**(2):977–991. https://doi.org/10.1104/pp.19.00752

Zhu J, Brown KM, Lynch JP. Root cortical aerenchyma improves the drought tolerance of maize (*Zea mays* L.). Plant Cell Environ. 2010:**33**(5):740–749. https://doi.org/10.1111/j.1365-3040.2009.02099.x

Zhu J, Mickelson SM, Kaeppler SM, Lynch JP. Detection of quantitative trait loci for seminal root traits in maize (*Zea mays* L.) seedlings grown under differential phosphorus levels. Theor Appl Genet. 2006:**113**(1):1–10. https://doi.org/10.1007/s00122-006-0260-z

Downloaded from https://academic.oup.com/plphys/advance-article/doi/10.1093/plphys/kiad213/7117337 by INRA AVIGNON user on 24 April 2023